Stochastic Fluid Dynamic Model and Dimensional Reduction

Valentin Resseguier, Etienne Mémin, Bertrand Chapron

International Symposium
On Turbulence and Shear Flow
Phenomena (TSFP-9)
June 30 - July 3, 2015 *Melbourne, Australia*

STOCHASTIC FLUID DYNAMIC MODEL AND DIMENSIONAL REDUCTION

Valentin Resseguier
Fluminance research group
INRIA
35042 Rennes, France
valentin.resseguier@inria.fr

Etienne Mémin
Fluminance research group
INRIA
35042 Rennes, France
etienne.memin@inria.fr

Bertrand Chapron
Laboratoire d'Océanographie Spatiale
IFREMER
29280 Plouzané, FRANCE
Bertrand.Chapron@ifremer.fr

ABSTRACT

This paper uses a new decomposition of the fluid velocity in terms of a large-scale continuous component with respect to time and a small-scale non continuous random component. Within this general framework, a stochastic representation of the Reynolds transport theorem and Navier-Stokes equations can be derived, based on physical conservation laws. This physically relevant stochastic model is applied in the context of the POD-Galerkin method. In both the stochastic Navier-Stokes equation and its reduced model, a possibly time-dependent, inhomogeneous and anisotropic diffusive subgrid tensor appears naturally and generalizes classical subgrid models. We proposed two ways of estimating its parametrization in the context of POD-Galerkin. This method has shown to be able to successfully reconstruct energetic *Chronos* for a wake flow at Reynolds 3900, whereas standard POD-Galerkin diverged systematically.

1 Introduction

Modeling accurately and understanding high Reynolds flow is a main issue in current researches. Indeed, beyond economic applications, turbulence needs still to be deeper understood. A classical way of modeling 3D turbulence consists to rely on the Boussinesq "eddy viscosity" assumption. However, the Eddy Viscosity matrix or coefficient and its temporal and spatial dependence has to be determined. In many cases, this is done empirically and/or using scaling assumptions. There may be mentioned LES (Lesieur & Metais (1996), Pope (2010)), or RANS (Wilcox (1988)).
The study Mémin (2014) and this paper follow another approach. The aim is to make appear naturally a physically based subgrid-tensor through a stochastic representation. In this approach, the small-scale velocity is assumed to be random and partially decorrelated in time. Using Stochastic Calculus , one can prove a stochastic representation of the so-called Reynolds transport theorem. Afterward, this theorem applied to momentum, and the 2^{nd} Newton Law leads to a stochastic version of Navier-Stokes equations.
For some industrial applications, the resolution of a large-scale system of Navier-Stokes equations (such as LES or RANS) may be even too time consuming. A solution to alleviate this issue consists to derive a model of reduced dimension, as in the case of the Proper Orthogonal Decomposition (POD) (Holmes *et al.* (1998)). It is composed of a finite set of coupled ordinary differential equations which describe the time evolution of the spatio-temporal decomposition of the velocity fields. However, keeping a too small number of modes ignores the small-scale contributions. Therefore, it usually destabilizes the system. To overcome this issue, some authors add empirically, to the reduced model, an Eddy Viscosity term (Aubry *et al.* (1988) , Rempfer & Fasel (1994), Östh *et al.* (2014), Protas *et al.* (2014)). Other authors (Carlberg *et al.* (2011)) perform non-linear Galerkin methods, with the same spatial modes. This leads to another form of the reduced model, that will not be investigated in this paper.
In our approach, the unresolved temporal modes are assumed to be random and decorrelated in time whereas the resolved one are deterministic. According to our stochastic Navier-Stokes model, an explicit sub-grid tensor appears both in the PDE and in the associated reduced model. The parameters of this sub-grid tensor can then be estimated on the residual velocity, through a statistical estimator. As we will see it, this subgrid tensor successfully stabilizes the reduced system.
The papers is organized as follow. The second section explains the stochastic Fluid Dynamics model, on which we rely. The third one presents our POD based reduced model under uncertainty. The fourth section presents some numerical results and comparisons. Finally, the last section concludes and gives perspectives.

2 The proposed stochastic model

This article will use an Eulerian stochastic representation of the velocity and tracer evolution law, as proposed in Mémin (2014). In most of classical stochastic representation of the Navier-Stokes equations, some parameters of

the deterministic model are randomized. Here, on the contrary, a random component, encoding an uncertainty on the velocity expression, is added to the Lagrangian velocity before any model derivation. Thanks to this decomposition, one can derive a stochastic representation of the so-called Reynolds transport theorem, cornerstone of the deterministic fluid dynamic theory. Applying this theorem to encode the conservation of mass and momentum transported by the random flow and assuming a dynamical balance similar to the 2^{nd} Newton law, enable us to exhibit a stochastic Navier-Stokes representation. This flow dynamics is hence derived in a very similar way as the deterministic one. Before describing in deeper details the form of this evolution law, we first present the stochastic flow representation we will deal with, and the corresponding Reynolds transport theorem.

2.1 Stochastic flow

In a Lagrangian stochastic picture, the infinitesimal displacement associated to the trajectory X_t of a particle is noted:

$$\mathrm{d}X_t = w(X_t,t)dt + \sigma(X_t,t)\mathrm{d}B_t \tag{1}$$

Function B_t denotes a d-dimentional Brownian function[1] and the resulting d-dimensional random field, $\sigma(x,t)dB_t$, is a centered Gaussian random field correlated in space and uncorrelated in time with covariance tensor:

$$Q_{ij}(x,y) = \sum_{k=1}^{d} \int_\Omega \breve{\sigma}^{ik}(x,y',t)\ \breve{\sigma}^{jk}(y',y,t)\mathrm{d}y'\delta(t-t')\mathrm{d}t \tag{2}$$

In the following we will note the diagonal of the covariance tensor as: $a(x) = Q(x,x)$. This tensor that will be referred to as the variance tensor is a symmetric positive definite matrix at all spacial points, x. This quantity corresponds to the time derivative of the so-called quadratic variation process:

$$a(x)\mathrm{d}t = \mathrm{d}\left\langle \int_0^t \sigma(x,s)\mathrm{d}B_s, \left(\int_0^t \sigma(x,r)dB_r\right)^T \right\rangle \tag{3}$$

$$= \sigma(x)\sigma(y)^T\mathrm{d}t \triangleq \int_\Omega \breve{\sigma}(x,z)\breve{\sigma}^T(x,z)\mathrm{d}z dt \tag{4}$$

The notation $\langle f,g\rangle$ stands for the quadratic cross-variation process of f and g. This central object of Stochastic Calculus can be interpreted as the covariance of time increments $d_t f$ and $d_t g$ along time. Furthermore, $\langle f,g\rangle = 0$ if f or g is differentiable w.r.t. (with respect to) time.
The drift term, w, of Lagrangian expression (1), represents the large-scale part of the velocity. It can be random but it is continuous w.r.t. time, since it varies slowly with time. At high Reynolds number, the small-scale velocity component lives at a much thinner time-scale than the former. This actual physical small-scale velocity is continuous w.r.t. time. But, the time sampling used for large-scale modeling or associated to the observation frame rate is often much bigger than the turn over time of the smallest eddies. Thus, at this time sampling, the smallest scales appear discontinuous w.r.t. time. Therefore, we model them through a random field uncorrelated in time.

[1] Formally it is a cylindrical I_d-Wiener process (see Da Prato & Zabczyk (1992) and Prévôt & Röckner (2007) for more information on infinite dimensional Wiener process and cylindrical I_d-Wiener process).

2.2 Stochastic representation of the Reynolds-transport theorem

Thanks to the decomposition (1), it is possible to derive a stochastic representation of the so-called Reynolds transport theorem (Mémin (2014)):

$$d_t \int_{V(t)} q(x,t)dx = \int_{V(t)} \left(d_t q + \nabla\cdot(q\,(w^* dt + \sigma dB_t)) - \nabla\cdot\left(\frac{a}{2}\nabla q\right)dt\right)dx \tag{5}$$

where $V(t)$ is a volume of fluid transported by the flow and:

$$w^* \triangleq w - \frac{1}{2}(\nabla\cdot a)^T + \sigma(\nabla\cdot\sigma)^T \tag{6}$$

A physical conservation of an extensive property, $\int_{V(t)} q$, such as mass or intern energy (neglecting diabatic and compressive effects) leads to the evolution of an intensive property, q :

$$d_t q + \nabla\cdot(q\,(w^* dt + \sigma dB_t)) = \nabla\cdot\left(\frac{a}{2}\nabla q\right)dt \tag{7}$$

If w is deterministic, the evolution of all the statistical moments of the intensive property can be formalized through it. For instance, the equation of the expectation, $\bar{q}$, is:

$$\frac{\partial \bar{q}}{\partial t} + \nabla\cdot(\bar{q}w^*) = \nabla\cdot\left(\frac{a}{2}\nabla\bar{q}\right) \tag{8}$$

The equation of the evolution of $\bar{q}$ is a classical advection-diffusion equation. The expectation, $\bar{q}$, is advected by the effective drift, w^*, (skew diffusion (Vallis (2006))) and undergoes a diffusion through the point-wise symmetric positive-definite tensor $\frac{a}{2}$. This advection-diffusion equation, derived from physical laws, has the same form than widely used large-scale advection-diffusion equation setup through an Eddy Diffusivity assumption (Vallis (2006), Kraichnan (1987)). However, unlike most of classical models, the subgrid diffusion we get is time-dependent, anisotropic and inhomogeneous.
In Stochastic Calculus theory, each function $f(t)$ can be decomposed uniquely into the sum of a smooth component (differentiable) $\int_0^t f_1(t)dt$ and a non differentiable one $\int_0^t f_2(t)dB_t$. For a constant density ρ, equation (7) for $q=\rho$ and the uniqueness of the decomposition leads to:

$$0 = \nabla\cdot\sigma \tag{9}$$

$$0 = \nabla\cdot w^* = \nabla\cdot\left(w - \frac{1}{2}(\nabla\cdot a)^T\right) \tag{10}$$

2.3 Stochastic Navier-Stokes model

Similarly to the Newton 2^{nd} law, a dynamical balance, between the temporal differentiation of the stochastic momentum, ρdX_t, and general stochastic forces action, is assumed. This leads, applying (5) to ρdX_t and ρ, to a stochastic Navier-Stokes representation.
To derive this stochastic dynamical model, in Mémin

(2014), it is assumed that w is differentiable w.r.t. time, which corresponds to a time scale separation assumption. Moreover, regarding to our application case, we will assume that the density ρ is constant. These assumptions leads to the incompressible Navier-Stokes model, for the smooth velocity component:

$$\frac{\partial w}{\partial t} + \mathscr{P}\left((w^* \cdot \nabla)w\right) = \mathscr{P}\left(\frac{1}{\rho}\tau(w)\right) + g + \nu\triangle w \quad (11)$$

where

$$\frac{1}{\rho}\tau_k(w) = \nabla \cdot \left(\frac{a}{2}\nabla w_k\right) \quad (12)$$

$$w^* = w - \frac{1}{2}(\nabla \cdot a) \quad (13)$$

$$\mathscr{P} \stackrel{\triangle}{=} \mathbb{I}_d - \triangle^{-1}\nabla\nabla^T \quad (14)$$

Expression (11) can be seen as a generalization of several classical turbulence model. For instance, if the (divergence-free) small-scale infinitesimal displacement σdB_t is homogeneous, the subgrid tensor simplifies to $\tau(w) = \rho\frac{a}{2}\triangle w$. Therefore, we retrieve the simplest expression of the Boussinesq assumption, with a constant Eddy Viscosity given by $\frac{a}{2}$. In a more general case, the effective advection does not affect the energy budget and the subgrid tensor τ is dissipative, as in a 3D direct energy cascade.
Equations (5) and (11) provides the foundations of a physically relevant stochastic Fluid Dynamics framework. In this paper, we will rely on it for the construction of reduced order dynamical systems.

3 Stochastic POD-ROM

Dimensional reduction are methods allowing simplification of partial differential equations (PDE), using dedicated basis specified from observed data. The Proper Orthogonal Decomposition (POD) is one of these methods. However, classical POD reduced order models (ROM) often suffers from stability issues. Our stochastic version of the POD-ROM helps overcoming this drawback. After introducing some notations, we explain how our model is derived. Then, we propose solutions to fix the simulation time step and for estimating the uncertainty variance tensor.

3.1 Classical model reduction using POD

In POD method, the velocity u is approximated by a linear combinations of n modes (Holmes *et al.* (1998)):

$$u(x,t) \approx \sum_{i=0}^{n} b_i(t)\phi_i(x) \text{ with } n \ll N \quad (15)$$

The functions $(\phi_i(x))_{1\leqslant i\leqslant N}$ constitute the spatial modes. They are referred to as *Topos* and are computed from a Karunen-Loeve decomposition on a series of available velocity snapshots. The *Topos* are sorted by decreasing order of the snapshots covariance eigenvalues: $\lambda_1 > ... > \lambda_N$, with N the number of observed snapshots. The $(b_i(t))_{1\leqslant i\leqslant N}$ correspond to the temporal modes or *Chronos*. Function ϕ_0 is the time average velocity and $b_0 \stackrel{\triangle}{=} \lambda_0 \stackrel{\triangle}{=} 1$. The time-space evolution equation of u (a PDE) is then expressed as the time evolution equations (a finite set of coupled ODEs) of *Chronos*. Because of the advection non-linearity, the temporal modes strongly interact with each others. In particular, even though the original model (with $n = N$) is computationally stable for moderate Reynolds number, the reduced one is not, in general. The method, we propose in the next section, allows us to tackle these drawbacks.

3.2 Stochastic reduced order model

To overcome the difficulties explained previously, we proposed to use our stochastic Navier-Stokes model, instead of the classical Reynolds average Navier-Stokes equation. Let us outline that both systems address the same Physics. They both rely on mass and momentum conservation and differ only on the way they are taking into account small-scale missing information.
To tackle the problem of modes interactions, Mémin (2014) proposed to decompose u as follow: $udt = wdt + \sigma dB_t$ with $w = \sum_{i=0}^{n} b_i\phi_i$ (projection on the truncated subspace) and $\sum_{i=n+1}^{N} b_i\phi_i dt$ a realization of σdB_t (projection on the complementary "small-scale" subspace). Since $\nabla \cdot u = 0$, for all i, $\nabla \cdot \phi_i = 0$ and, then, $\nabla \cdot w = 0$. The drift, w, follows the incompressible stochastic Navier-Stokes equation (11). Projecting this equation along ϕ_i leads to:

$$\frac{db_i}{dt} = i_i + \left(l_{\bullet i} + \breve{f}(a)_{\bullet i}\right)^T b + b^t c_{\bullet\bullet i} b \quad (16)$$

where the coefficients i, $\breve{f}(a)$, l and c are computed through projection on the *Topos* basis functions of the terms of (11). Let us note that $\breve{f}(a)$ is linear and is the only function which depends on the variance tensor a. This system includes a natural small-scales dissipation mechanism, through the tensor τ. To fully specify this system, we need to estimate the quadratic variance tensor a. This main issue is developed in subsection 3.4. But before that we elaborate further on the choice of a characteristic time step related to the truncation operated.

3.3 Choice of the time step

For several applications, the simulation of the most energetic large-scale components of the solution is sufficient. However, this simulation needs to be fast, meaning both a low complexity evolution model and a large time step. Our stochastic model enables to reach both goals.
Indeed, as long as the resolved modes, which represent w, are differentiable w.r.t. time, our stochastic reduced model is valid. Thus, we choose the biggest time step ensuring that these modes remains smooth. Qualitatively, the smallest time scale of the resolved *Chronos* and their derivatives is a good target. It is associated to the frequencies of their last energetic Fourier modes. Quantitatively, the Shannon-Nyquist theorem provides us a natural upper bound to fix this time step. If the resolved POD modes and their evolution equations are not affected by aliasing phenomena, the required smoothness is assumed to be reach. Since the evolution equations are quadratic, a sufficient condition for the necessary smoothness is:

$$\frac{1}{\Delta t} \geqslant 4\, max_{i\leqslant n}\left(f_{max}(b_i)\right) \quad (17)$$

where $f_{max}(b_i)$ is the maximum frequency of the i-th mode. Of course, aliasing will occur in the unresolved temporal

modes, associated to smaller time scales. However, our stochastic model is built from a decorrelation assumption of the small-scale unresolved part of the velocity. A strong subsampling of these components strengthen thus the decorrelation property of these modes.

3.4 Estimation of the uncertainty variance tensor

After having estimated the *Topos* and fixed the time step, we need to estimate the uncertainty variance tensor a. This estimation will enable getting a full expression of the dynamical coefficients of the *Chronos* evolution equations (16). To that end additional modeling assumptions must be imposed. The first natural hypothesis consists to assume an uncertainty field that is stationary in time. In this stationary case, the uncertainty variance tensor is constant in time (and spatially non-homogeneous).

3.4.1 The uncertainty variance tensor is constant in time This case corresponds to the assumption used in Mémin (2014). To understand the consequence of this hypothesis, we recall that $\frac{a}{\Delta t}$ is the variance of the residual velocity $u-w$. This function is decorrelated in time. The snapshots are hence independent. Therefore, the variance, $\frac{a}{\Delta t}$, can be computed averaging the snapshots $(u-w)(u-w)^T(t_i)$.

3.4.2 The uncertainty variance tensor is in the span of the Chronos Assuming constant value for the tensor $a(x)$ means that the turbulence is not intermittent. In the context of POD, it would mean that all the unresolved modes have a constant variance. It is a good first approximation. But, one can wonder whether it is possible to do better.

If the uncertainty variance tensor a does depend of time, the estimation is more involved, since only one realization of the small scale velocity, $(u(x,t)-w(x,t))$, is available. However, Stochastic Calculus theory helps to overcome this difficulty. Indeed, at a fixed point x, it allows to estimate the coefficients, $z_i(x)$, of the tensor, $a(x,t)$, in basis of function of time (Genon-Catalot *et al.* (1992)). If we choose the *Chronos* reduced basis:

$$a(x,t) = \sum_{i=0}^{d} b_i(t) z_i(x) \tag{18}$$

Then, the coefficients can be estimated as:

$$\begin{aligned} z_i(x) &= \int_0^T \frac{b_i(t)}{T\lambda_i} a(x,t)dt \\ &= \int_0^T \frac{b_i(t)}{T\lambda_i} d\left\langle \int_0^t \sigma(x,t')dB_{t'}, \left(\int_0^t \sigma(x,t')dB_{t'}\right)^T \right\rangle \\ &= \lim_{\Delta t\to 0} \sum_{t_k=0} \frac{b_i(t_k)}{T\lambda_i} \sigma(x,t_k)dB_{t_k} (\sigma(x,t_k)dB_{t_k})^T \\ &\approx (\Delta t)^2 \sum_{t_k=0}^{T} \frac{b_i(t_k)}{T\lambda_i} (u-w)(x,t_k)((u-w)(x,t_k))^T \end{aligned} \tag{19}$$

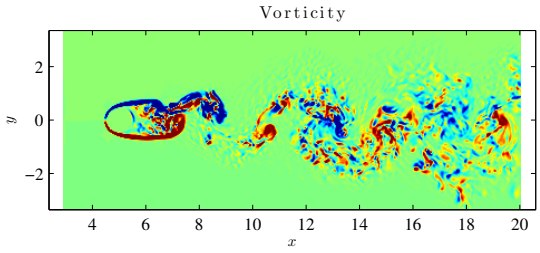

Figure 1. Vorticity along z at the first time step in the horizontal section $z=0$.

Thus, (16) stays a quadratic autonomous system:

$$\frac{db_i}{dt} = i_i + l_{\cdot i}^T b + b^T (c_{\cdot\cdot i} + f_{\cdot\cdot i})\, b \tag{20}$$
$$\text{with } f_{pqi} \stackrel{\triangle}{=} \check{f}_{qi}(z_p)$$

4 Numerical results

The different variations of the approach proposed have been assessed and compared numerically on numerical data, from a LES simulation of a wake behind a cylinder, at Reynolds 3900 (Parnaudeau *et al.* (2008)).

4.1 Characteristics of the data

The fluid is incompressible. At $x=0$, there is a constant velocity $U=1$ directed along $x>0$. At $(x,y)=(5,0)$, there is motionless cylinder with an axis along the z axis. In permanent regime, it creates a Von Kármán vortex street. Figure 1 shows the z component of the vorticity on horizontal section of the fluid. Kelvin-Helmholtz instabilities at the top right and bottom right of the cylinder can also be observed just before the vortex creation zone. At this Reynolds, the turbulence is relatively important. Thus, in the context of POD, the *Chronos* live at different time scale. It makes our stochastic model, based on a separation between smooth and highly oscillating parts of the velocity, more relevant. In the study, we use $N=251$ time steps to observe 3 vortex shedings.

4.2 Reconstruction of Chronos

To reconstruct the *Chronos*, the reduced order dynamical system (20) is used. The modes mean energy, $(\lambda_i)_{1\leqslant i\leqslant n}$, and the *Topos*, $(\phi_i)_{0\leqslant i\leqslant n}$, are computed from the whole sequence of snapshots ($N=251$). As for the initial condition, we used the referenced values of the Chronos computed directly from the scalar product of the initial velocity with the *Topos*. Then, regarding the *Chronos* spectra, an optimal time sub-sampling is chosen, as explained in subsection 3.3. Afterward, using the residual velocity and possibly the *Chronos*, the variance tensor, a, or its decomposition is estimated. The coefficients of the reduced order dynamical system of *Chronos*, (20), are computed, using discrete derivation schemes and integration. Finally, the *Chronos* trajectories are simulated, integrating (20) with a 4-th order Runge-Kutta method, with $b^{ref}(t=0)$ as initial condition.

Figure 2 shows an example of the reconstruction of the *Chronos* for $n=10$ with the classical POD method (blue plot) and our method with a variance tensor defined as a linear combination of *Chronos* (red plot). The reference $(b_i^{ref})_{1\leqslant i\leqslant n}$ (black plot) are superimposed for comparison

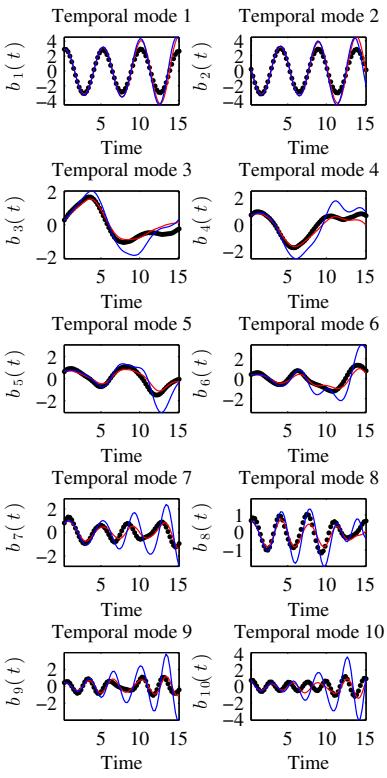

Figure 2. Reconstruction of the 10 first modes (n=10) with a variance tensor expressed as a linear function of the *Chronos*. The black plots are the observed references. The blue lines corresponds to the solutions computed with a standard POD-Galerkin whereas the red ones are computed with the stochastic representation, without any corrective coefficient. The initial condition, at $t = 0$, is common.

purpose. It can be observed that our model follows the references quite well whereas the deterministic model blows up very quickly. Let us point out that here both reduced models are parameter free. No constant has been tuned to adapt any viscosity model.

Figure 3 shows the error of the solution along time. Approximating the square of the actual unresolved *Chronos* by the time average of their square, the error is defined as follows:

$$err(t) = T\frac{\left\|u^{ref}-u\right\|_{L^2(\Omega)}}{\left\|u^{ref}\right\|_{L^2(\Omega\times[0,T])}} \approx \left(\frac{\sum_{i=1}^{n}\left(b_i^{ref}-b_i\right)^2+\sum_{i=n+1}^{N}\lambda_i}{\|\phi_0\|^2_{L^2(\Omega)}+\sum_{i=1}^{N}\lambda_i}\right)^{1/2} \quad (21)$$

which is greater than the minimal error associated to the modal truncation:

$$err(t) \geqslant \left(\frac{\sum_{i=n+1}^{N}\lambda_i}{\|\phi_0\|^2_{L^2(\Omega)}+\sum_{i=1}^{N}\lambda_i}\right)^{1/2} \quad (22)$$

Equation (21) defines the criterion error plotted in Figure 3, whereas (22) constitutes a lower bound of this error.

In Figure 3, we show the error, obtained for the standard POD Galerkin model without subgrid dissipative term, and our model for a variance tensor which is either fixed constant along time or expressed as a linear combination of the *Chronos*. The doted line is the minimal error associated to the reduced subspace truncation error. The black solid line is the error considering only the time mean velocity – if we set all the *Chronos* to 0. In this case:

$$err_{|b=0}(t) \approx \left(\frac{\sum_{i=1}^{N}\lambda_i}{\|\phi_0\|^2_{L^2(\Omega)}+\sum_{i=1}^{N}\lambda_i}\right)^{1/2}$$

This term does not constitute an upper bound of the error. However, if this limit is crossed, it means that the model is completely useless. In Figure 2, knowing that the y axis has a log scale, one can see the exponential divergence of the standard POD reduced order (in blue). Conversely, our methods, based on a physically relevant stochastic representation of the small scale component, work quite well, even though no learning or tuning was used. There is only a slight difference between a constant and a linear representation of the variance tensor. A drawback of the second method is that $a(x,t)$ is not ensured to be a positive definite matrix. When the number of modes increases, the basis, $(b_i)_{0\leqslant i\leqslant n}$, used for the projection of the tensor, a, is larger. Thus, the projection approximates better the identity, and the estimation of $a(x,t)$ becomes closer to a positive matrix and close to real value of the tensor. This may explain the difference between the two methods.

Whatever their differences, both methods provide very encouraging result, as such representations enables clearly the construction of autonomous subgrid models. This constitutes an essential point for the devising of autonomous reduced order dynamical systems.

5 Conclusion

In this paper, a Fluid Dynamics model, built from fundamental physical principles applied to a stochastic representation of the flow, has been used. In this representation, the fluid velocity is random and partially decorraleted in time. This time decorrelation can be interpreted as coming from a subsampling in time of a fast oscillating part of the velocity. In this framework, mass and momentum conservation principles can be constituted from Stochastic Calculus to derive a complete fluid flow dynamics model. This framework brings a strong theoretical support to classical empirical models, while generalizing them through the incorporation of an anisotropic, inhomogeneous and time-dependent diffusion. Thanks to our stochastic representation of fluid dynamics, a reduced model, describing the resolved modes evolution, has been derived. This model takes explicitly into account the unresolved modes influence. Since our model enables to deal with aliasing effects, we have chosen a time step as big as possible to improve the efficiency of the reduced model simulation. A criterion based on Shannon-Nyquist theorem has been proposed to set the time step. Two different methods have been proposed to estimate the variance tensor. The first one relies on the assumption of a constant variance tensor along time, whereas the second one decomposes this tensor as a linear combination of the *Chronos* basis. From both methods, closed autonomous reduced systems have been derived. Finally, both methods have been tested on numerical data

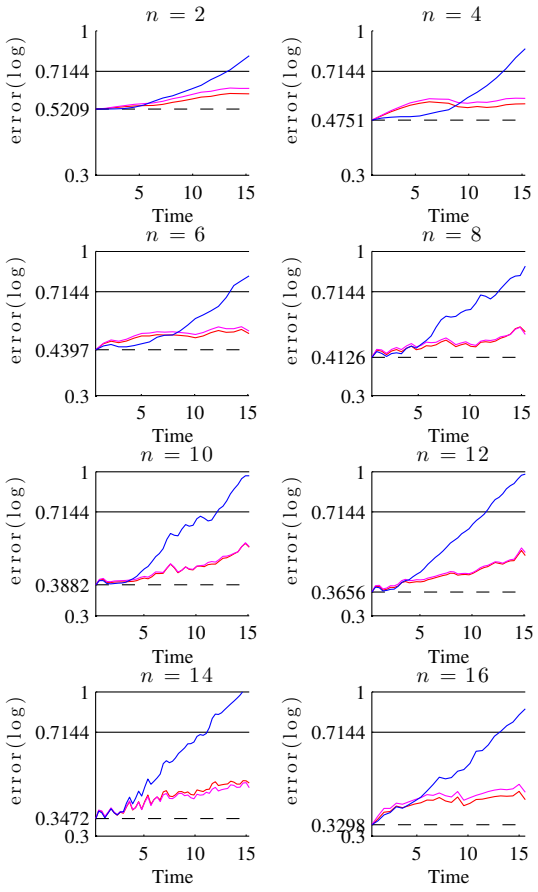

Figure 3. Normalized error for n = 2, 4, 6, 8, 10, 12, 14 and 16 modes. The error is normalized by the energy of the solution: $\sum_{i=1}^{N} \lambda_i$. The blue line corresponds to the standard POD Galerkin. The red one stands for our model with a constant variance tensor along time. The magenta one represents our model with linear representation of the variance tensor. The doted line indicates the error associated to the mode truncation : $\sum_{i=n+1}^{N} \lambda_i$. The black solid line is the error considering only the time mean velocity.

from LES simulation at Reynolds 3900 of wake flow. The two kinds of reduced models have been compared to POD Galerkin reduced system. The standard reduced system exhibits very fast diverging trajectories. At the opposite, our models have shown to provide much better results without any parameter tuning.

Those results are very encouraging. However, a lot of improvements are possible and may be considered. Here, the small-scale velocity has been assumed to be constant in time or linear in the temporal modes. But, one can also assumes that it is a quadratic or a cubic function of the temporal modes. Another improvement can be brought by time sampling adapted to each resolved modes, in order to make the most of the time-decorraleted unresolved velocity explicit influence. Finally, it could be suitable to remove the differentiability assumption for the large-scale drift, w. This would enable uncertainty quantification and to take into account partially time-correlated sub-grid velocity components influence, such as energy back-scatterings.

Acknowledgements

We are thankful to the ANR Geronimo which supported this work. The authors also would like to kindly thank Johan Carlier and Dominique Heitz, for providing data and their expertise in physical interpretations.

REFERENCES

Aubry, N., Holmes, P., Lumley, J. L & Stone, E. 1988 The dynamics of coherent structures in the wall region of a turbulent boundary layer. *Journal of Fluid Mechanics* **192**, 115–173.

Carlberg, K., Bou-Mosleh, C. & Farhat, C. 2011 Efficient non-linear model reduction via a least-squares petrov–galerkin projection and compressive tensor approximations. *International Journal for Numerical Methods in Engineering* **86** (2), 155–181.

Da Prato, G. & Zabczyk, J. 1992 *Stochastic Equations in Infinite Dimensions*. Cambridge University Press.

Genon-Catalot, V., Laredo, C. & Picard, D. 1992 Nonparametric estimation of the diffusion coefficient by wavelets methods. *Scandinavian Journal of Statistics* pp. 317–335.

Holmes, P., Lumley, J. & Berkooz, G. 1998 *Turbulence, coherent structures, dynamical systems and symmetry*. Cambridge university press.

Kraichnan, R. 1987 Eddy viscosity and diffusivity: exact formulas and approximations. *Complex Systems* **1** (4-6), 805–820.

Lesieur, M. & Metais, O. 1996 New trends in large-eddy simulations of turbulence. *Annual Review of Fluid Mechanics* **28** (1), 45–82.

Mémin, E. 2014 Fluid flow dynamics under location uncertainty. *Geophysical & Astrophysical Fluid Dynamics* **108** (2), 119–146.

Östh, J., Noack, B., Krajnović, S., Barros, D. & Borée, J. 2014 On the need for a nonlinear subscale turbulence term in pod models as exemplified for a high-reynolds-number flow over an ahmed body. *Journal of Fluid Mechanics* **747**, 518–544.

Parnaudeau, P., Carlier, J., Heitz, D. & Lamballais, E. 2008 Experimental and numerical studies of the flow over a circular cylinder at reynolds number 3900. *Physics of Fluids* **20** (8), 085101.

Pope, S. 2010 Self-conditioned fields for large-eddy simulations of turbulent flows. *Journal of Fluid Mechanics* **652**, 139–169.

Prévôt, C. & Röckner, M. 2007 *A concise course on stochastic partial differential equations*, , vol. 1905. Springer.

Protas, B., Noack, B. & Östh, J. 2014 Optimal nonlinear eddy viscosity in galerkin models of turbulent flows. *arXiv preprint arXiv:1406.1912* .

Rempfer, D. & Fasel, H. 1994 Evolution of three-dimensional coherent structures in a flat-plate boundary layer. *Journal of Fluid Mechanics* **260**, 351–375.

Vallis, G. 2006 *Atmospheric and oceanic fluid dynamics: fundamentals and large-scale circulation*. Cambridge University Press.

Wilcox, D. 1988 Reassessment of the scale-determining equation for advanced turbulence models. *AIAA journal* **26** (11), 1299–1310.